Penerbit Akademia Baru

Journal of Advanced Research in Fluid Mechanics and Thermal Sciences

Journal homepage: www.akademiabaru.com/arfmts.html
ISSN: 2289-7879

Study on Selection of a Suitable Material and The Parameters for Designing a Portable Flat Plate Base-Thermal Cell Absorber (FPBTCA)

Muhammad Amin Harun[1], Zafri Azran Abdul Majid[2,*], Zairul Azrul Zakaria[1], Ahmad Faris Ismail[1], Sany Izan Ihsan[1], Kamaruzzaman Sopian[3], Ahmad Fadzil Sharol[4], Amir Abdul Razak[4]

[1] Kuliyyah of Engineering, International Islamic University Malaysia, Jalan Gombak, 53100 Kuala Lumpur, Malaysia
[2] Kuliyyah of Allied Health Sciences, International Islamic University of Malaysia, 25200 Bandar Indera Mahkota Kuantan, Pahang, Malaysia
[3] Solar Energy Research Institute, Universiti Kebangsaan Malaysia, 43600 Bangi Selangor, Malaysia
[4] Faculty of Mechanical Engineering Technology, Universiti Malaysia Pahang, 26600 Pekan, Malaysia

ARTICLE INFO

Article history:
Received 9 March 2021
Received in revised form 23 June 2021
Accepted 26 June 2021
Available online 28 July 2021

Keywords:
flat plate solar collector (FPSC); thermal cell absorber; absorber base collector

ABSTRACT

Several types of flat plate solar collectors have been designed and developed with various technical parameters involved in the design. The limitations of a flat plate solar collector are energy storage and design of flat plate absorber height and weight. An investigation on the effect of flat plate absorber-collector material, glass thickness, air gap distance and flat plate absorber base collector thickness on the performance of solar thermal collectors was conducted in this work. The results obtained will be used as the base to develop thermal cell application on flat plate solar collector. The experiment was performed using a solar simulator with solar radiation of 450 W/m^2 and 750 W/m^2. The results showed that 2.0 mm glass thickness yielded maximum flat plate absorber temperature (88.1 °C at t = 600 s), high heat gain rate (0.097 °C/s), and highest total heat gain (1207.33 J). The results also revealed that the air gap distance of 10.0 mm achieved maximum flat plate absorber temperature (64.6 °C at t = 600 s), highest heat gain rate (0.058 °C/s), and highest total heat gain (4750.92 J). The stainless-steel thermal cell absorber thickness of 1.0 mm yielded thermal cell absorber temperature (76.2 °C at t = 600 s) and high heat gain rate (0.08 °C/s). The aluminum flat plate base absorber achieved the highest flat plate absorber temperature (67.2 °C at t = 600 s) and the highest heat gain rate (0.062 °C/s). Using double glass as glass cover increased the flat plate absorber temperature (76.3 °C at t = 600 s) and highest heat gain rate (0.077 °C/s). This research aims to produce a flat plate absorber with better energy storage, and with the performance of the stainless-steel plate absorber better than aluminum of the same thickness. Although the stainless-steel flat plate absorber-collector showed a lower temperature than aluminum, it had a higher temperature drop than the latter.

* *Corresponding author.*
E-mail address: zafriazran@yahoo.com

https://doi.org/10.37934/arfmts.85.1.7192

1. Introduction

Solar energy is a renewable energy source [1], and its usage could mitigate environmental impacts [2]. The increasing application of solar energy as alternative energy is also due to increasing fossil fuel prices [3]. Solar energy has been used in solar thermal technology such as solar air-heating system, solar water-heating system, photovoltaic system, and solar thermal system [4]. One example of solar thermal technology application is drying of agricultural products [5], where the products are dried with a solar dryer to increase shelf-life [6] and expedite the time of drying [7]. Basically, the temperature of drying chamber for drying agricultural products is between 50°C to 60°C [8]. The solar dryer objective is to reduce agricultural moisture content so that the physical and chemical properties could be minimised during the storage to increase shelf-life [9].

A solar thermal collector is used in the flat plate solar collector (FPSC) for drying. FPSC is used because of its low cost manufacturing, inexpensive maintenance [10, 11] and environmental friendliness. While, the evacuated solar collector addition of TiO2-nanoparticles was used to improved heat transfer in the system [12]. The components of a flat plate solar thermal collector comprise a glass cover, a flat plate absorber-collector, thermal energy storage [13] and insulation at the bottom side. Several design parameter criteria should be considered when designing a new FPSC, such as the flat plate absorber-collector material [14] and thickness [15], glass thickness, and air gap distance (between the absorber and glass). The performance of FPSC could be improved using the optimum FPSC design parameters. The material used for the flat plate absorber-collector is copper, aluminum, and stainless steel [16].

Previous researchers had focused on the design parameters that affected the performance of an FPSC. An experiment on a flat plate absorber material was conducted by Billy *et al.*, [17] who reported that aluminum flat plate absorber performed better than copper flat plate absorber. Another study indicated that the highest air temperature was achieved when the flat plate absorber thickness was 3 cm [18]. Meanwhile, Billy [19] reported that an aluminum absorber thickness of 2 mm was preferred for FPSC. The thickness of the flat plate absorber- collector significantly affects the thermal efficiency of an FPSC [20]. The fact absorber or influencing the solar energy absorber by the flat plate absorber-collector is the transmittance of heat through the glass cover to trap radiated heat from the flat plate absorber-collector [21]. The performance of FPSC could be improved by 7.6% with the use of a 4-mm thick glass as the glass cover [22].

Ghoneyem *et al.,* [23] experimented with three solar stills with different glass thicknesses; 3, 5, and 6 mm, and the result showed that the still with 3 mm glass thickness produced the highest production rates, up to 15.5%. Proper handling should be considered when using a thin glass cover for the FPSC. The air gap between absorber and glass functions is meant to trap heat loss from the flat plate absorber-collector. An insignificant augmentation was noted when the air gap between the absorber and the glass exceeded 5 cm [24]. Other results showed that the heat loss coefficient decreased when the air gap spacing decreased [25]. A study by Mintsa Do Ango *et al.,* [26] found that the air gap between the absorber and glass should be 10 mm for optimal performance. Another review showed that by using double glass the thermal efficiency was higher than single glass for flat plate solar water heater [27]. Previous studies have also proven that the design parameters could affect the FPSC performance.

The enhancement of flat plate solar collector (FPSC) could be done by improvement of thermal absorber-collector to increase the performance. The improvement of absorber thermal collector can be done by several criteria such as fins absorber, ribbed absorber, corrugated absorber, phase change material (PCM), porous media and nanofluids as the working fluid. Youcef Ali [28] found that use of fins on the absorber-collector could improve thermal performance and reduce pressure losses. Use of ribs attached to the flat plate absorber-collector could create uniform temperature and improve heat absorption [29]. Another improvement could be done by using corrugated absorber-collector to gain higher heat at higher temperature [30]. Kürklü *et al.,* [31] found that the section of absorber-collector could be filled with phase change material with high phase change temperature to increase efficiency. Use of porous metal foam on the absorber-collector could further improve the thermal performance of the flat plate solar collector [32]. A study by Hessein [33] concluded that nano particle size could give major effect to the efficiency performance of flat plate solar collector.

Therefore, this research aims to find a suitable material and thickness for flat plate base collector and thermal cell for Flat Plate Base-Thermal Cell Absorber (FPBTCA). This study also investigates the optimum parameters for glass thickness and air gap distance (between absorber-collector and glass cover) applicable for the Flat Plate Base-Thermal Cell Absorber (FPBTCA).

1.1 Heat Transfer and Thermal Resistance for Flat Plate Solar Collector (FPSC)

Figure 1 shows (a) Schematic diagram for heat transfer in single cover [34], (b) Thermal network based on resistance between plates and c) Thermal network based on conduction, convection and radiation resistance. Thermal network is used for a single cover flat plate solar collector (FPSC). T_p refers to temperature of flat plate solar collector, T_c is temperature of glass cover and T_a is ambient temparature, while S is incident solar radiation reduced by optical losses.

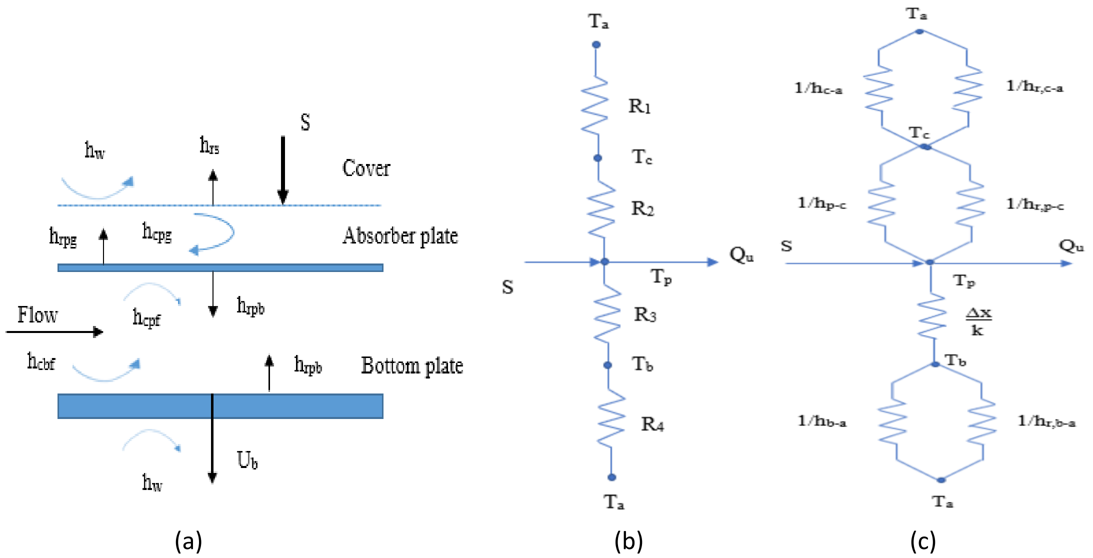

Fig. 1. (a) Schematic diagram for heat transfer in single cover [34] (b) Thermal network based on resistance between plates and (c) Thermal network based on conduction, convection and radiation resistance

The heat transfers for single cover are shown in Figure 1(a).

For the cover

$$\alpha_g S + h_{rpg}(T_p-T_g) + h_{cpg}(T_p-T_g) = (h_w - h_{rs})(T_g-T_a) \tag{1}$$

For the absorber plate

$$\alpha_p \tau_g S = h_{cpf}(T_p-T_f) + h_{cpg}(T_p-T_g) + h_{rpb}(T_p-T_b) + h_{rpg}(T_p-T_g) \tag{2}$$

For the flowing air

$$h_{cpf}\,(T_p\text{-}T_f) = h_{cbf}\,(T_f\text{-}T_b) + \frac{mcf}{w}\frac{\mathrm{dTf}}{dx} \tag{3}$$

Bottom plate

$$h_{cpf}\,(T_f\text{-}T_b) + h_{rpb}\,(T_p\text{-}T_b) = U_b(T_b\text{-}T_a) \tag{4}$$

The boundary conditions

$$T_f(x=0) = T_{fi},\ T_f(x=L) = T_{fo} \tag{5}$$

2. Devices Used in The Experiment

The FPSC was exposed to the solar simulator. The devices used in this experiment were selected based on their ability to conduct the experiment and gain data for analysis. An AT4208 Multi-Channel Temperature Meter (8-Channel, Applent Technology, China) and a pyranometer (Apogee Instruments, USA) were used to measure the temperature of the absorber's wall and solar radiation. For calibration purposes, the real-time solar radiation flux was measured using the TES-1333R Solar Power Meter (Datalogging, TES Electrical Electronic Corp., China). The readings recorded by the pyranometer and data logger were calibrated for their validity and reliability before conducting the experiment.

3. Methodology

The experiment was conducted indoor in a controlled environment. The details of each experiment conducted are explained in the following sub-sections. The data logger and the 8-channel Temperature Meter were used to record the data in the experiment. The temperature was recorded every 1 second using the data logger, comprising three units of thermocouple data loggers namely, T1, T2, and T3, to record the surface temperature of the flat plate absorber and glass. T4 is used to record the ambient temperature of the surrounding. The recorded data were analysed, and a graph was plotted. Charging process is defined as the exposure of FPSC under a solar simulator, while the discharging process is defined as the exposure of FPSC without the solar simulator. Charging process was done for 10 minutes under the solar simulator, and the discharging process was conducted by removing the solar simulator, and the process continued for another 10 minutes.

3.1 Evaluation of Flat Plate Absorber Material, Glass Thickness, Air Gap Distance and Flat Plate Absorber Base Collector Thickness

Figure 2 shows the experimental set-up of the study before the experiment. The figure represents the flat plate absorber material set-up, glass thickness, air gap distance, and flat plate absorber base collector thickness. The flat plate solar collector has a distance of 18 cm between the solar simulator. Figure 3 represents the flat plate solar collector diagram used in the experiment. The figure shows the top and side views of the flat plate solar collector diagram. The size of the flat plate absorber-collector used is 18.5 cm in width and 25.5 cm in length. The flat plate solar collector box size is 22.0 cm in width and 29.5 cm in length.

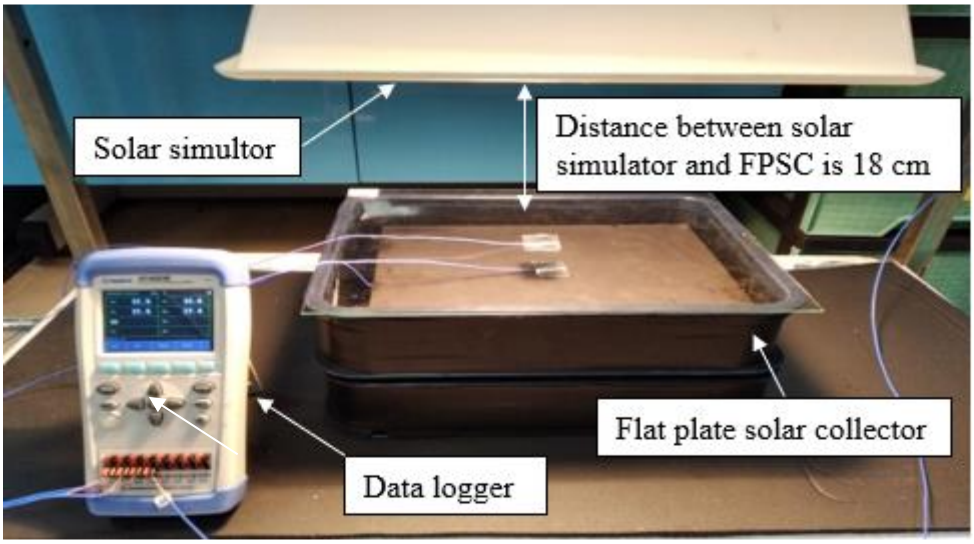

Fig. 2. Experimental set-up

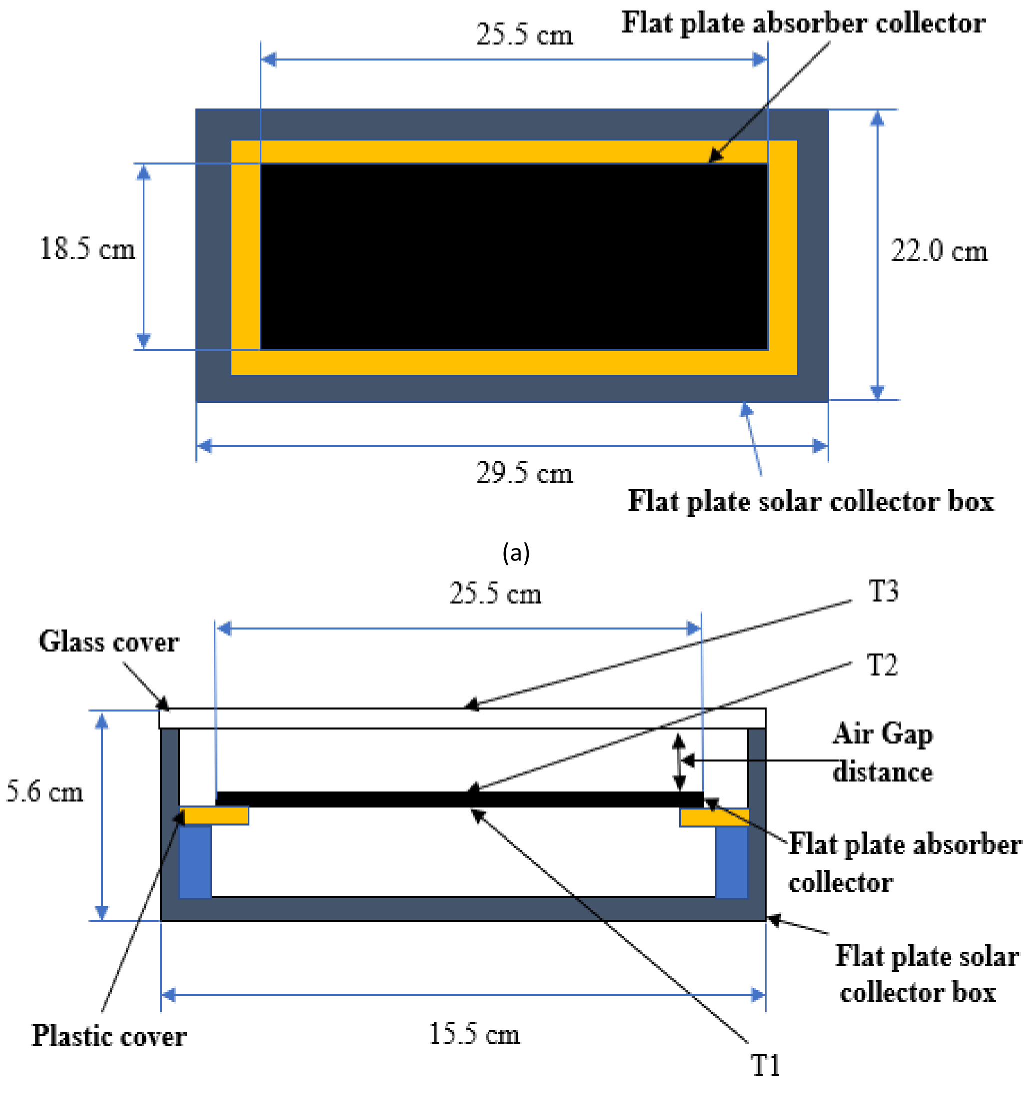

Fig. 3. (a) Top view and (b) Side view of flat plate solar collector diagram

3.2 Method to Evaluate Different Coating Surfaces and Thermal Cell Absorber

Figure 4 represents the experimental set-up of the experiment. The figure represents the set-up for different coating surfaces and different thermal cell absorbers. The data were recorded every 1 second using the data logger and the 8-channel Temperature Meter. The distance between the flat plate solar collector and solar simulator is 19 cm. Figure 5 shows the flat plate solar collector diagram used in the experiment. The figure shows the top and side views of the flat plate solar collector diagram. Flat plate absorber-collector size is 10.0 cm in width and 10.0 cm in length, and the flat plate solar collector box size is 15.5 cm × 15.5 cm.

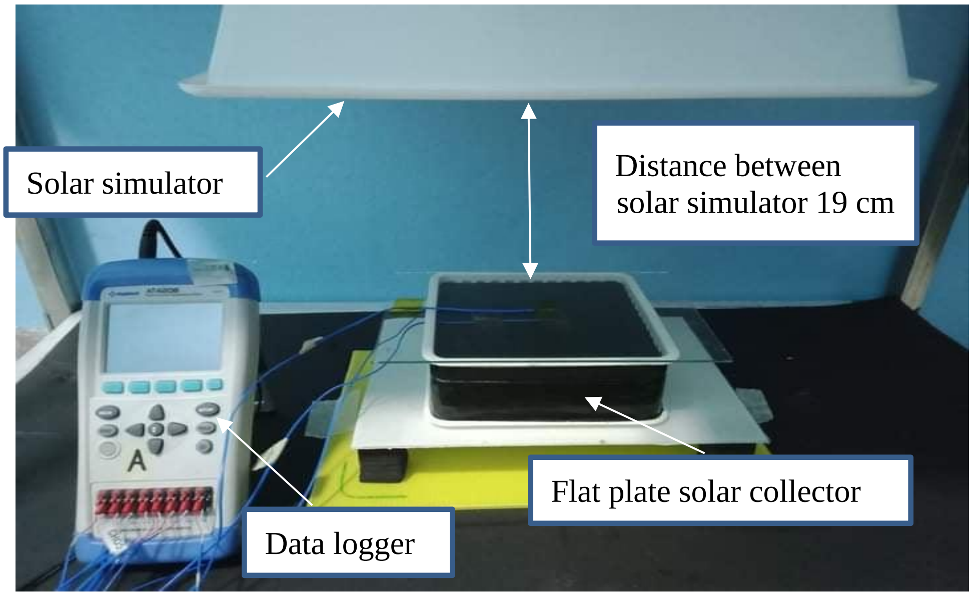

Fig. 4. Experimental set-up

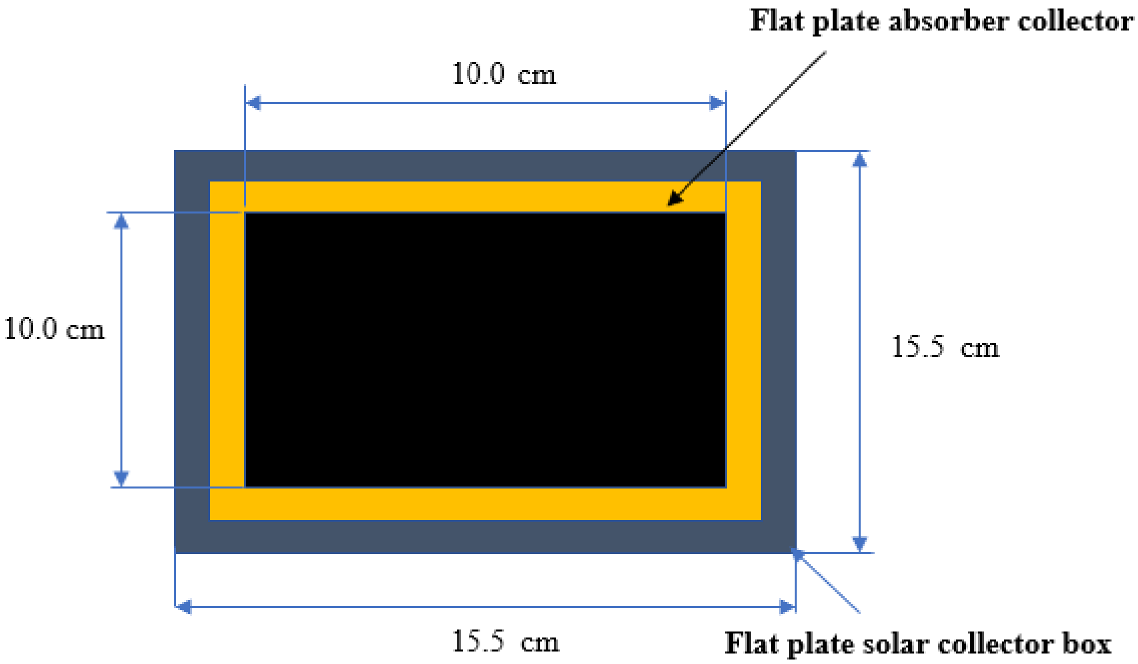

(a)

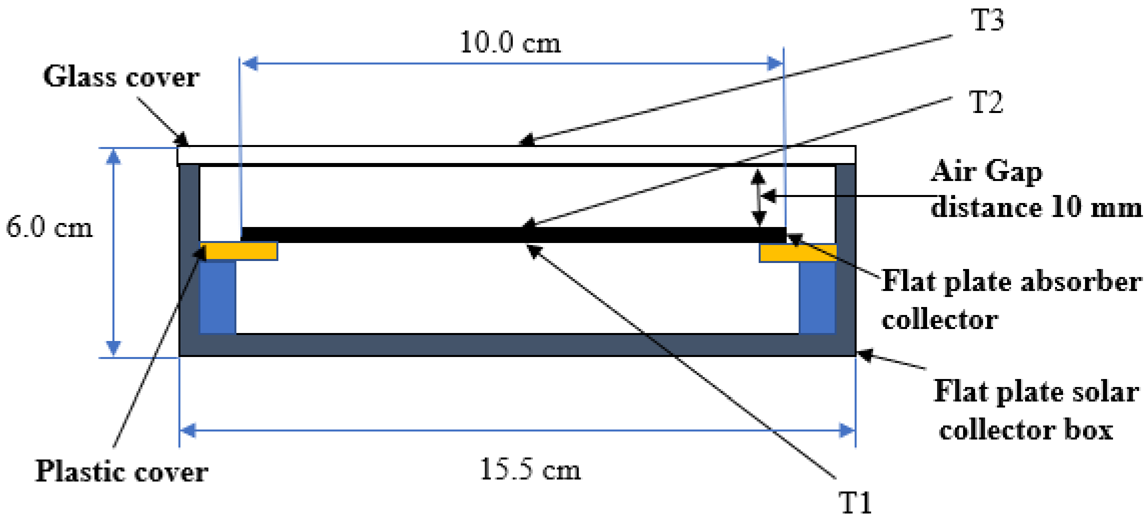

(b)

Fig. 5. (a) Top view (b) Side view of flat plate solar collector diagram

3.3 Selection of Flat Plate Absorber-Collector Materials

Solar simulator radiation of 450 W/m^2 was applied in this experiment. Table 1 shows the flat plate absorber materials configuration used in the experiment. Aluminum and stainless steel are used as the flat plate absorber-collector materials. The aluminum and stainless steel size is 18.5 cm × 25.5 cm, and the area is 471.75 cm^2. Flat plate absorber-collector thickness of 0.8 mm was selected for the configuration of both materials, and the weight is 0.101 kg and 0.271 kg for aluminum and stainless steel, respectively.

Table 1
Flat plate absorber materials configuration

Material	Size (WxL)(cm)	Area (cm^2)	Thickness (mm)	Weight (kg)
Aluminium	18.5 x 25.5	471.75	0.8	0.101
Stainless Steel	18.5 x 25.5	471.75	0.8	0.271

3.4 Coating and Non-Coating Surfaces

Aluminum flat plate absorber-collector with 0.5 mm thickness was used in the experiment to compare the coating surface and non-coating surface. The size of the flat plate absorber-collector is 10.0 cm in length and 10.0 cm in width and weighs 0.015 kg. Solar simulator radiation of 450 W/m^2 was applied in the experiment. Figure 6 shows the non-coated and coated flat plate thermal cell absorber used in this study. Matt black paint has been used for coating the surface of the aluminum flat plate absorber. The experiment was conducted for 5 minutes charging under solar radiation and 5 minutes of discharging by removing the solar simulator for 5 minutes.

(a) (b)

Fig. 6. (a) Non-Coated and (b) Coated for flat plate absober collector

3.5 Selection of Flat Plate Thermal Cell Absorber Thickness

The constant parameters used in this experiment were the air gap space and glass thickness. The flat plate absorber-collector and glass cover has an air gap space of 10.0 mm. Glass thickness of 2.0 mm was used in this experiment. Stainless steel 304 was used for the flat plate thermal cell absorber. Solar simulator used in this experiment has 450 W/m^2 radiation. Figure 7 presents the flow chart of the experiment executed. Three types of flat plate thermal cell absorbers of 0.5 mm, 1.0 mm and 2.0 mm thickness were used in this experiment. The weight of the flat plate thermal cell thickness of 0.5 mm, 1.0 mm and 2.0 mm is 0.038 kg, 0.073 kg and 0.172, respectively.

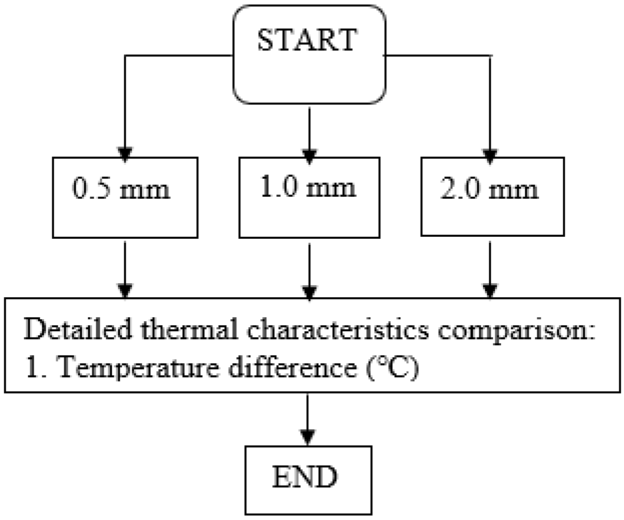

Fig. 7. Flow chart of the experiment with constant air gap space and glass thickness

3.6 Selection of Glass Thickness

The constant parameters used in this experiment were flat plate absorber thickness and the air gap space (air gap between the absorber and glass). Stainless Steel 304 flat plate absorber thickness is 1.2 mm, and its weight is 0.415 kg. The flat plate absorber-collector and glass cover has an air gap thickness of 10.0 mm. The solar simulator used in this experiment emits a constant rate of 750 W/m^2 radiation. The high solar radiation rate was meant to simulate the behavior of glass thickness. Figure

8 shows the flow chart of the experiment carried out. The glass thickness used in this experiment is 2.0, 3.0, 4.0, 5.0, and 10.0 mm, as top cover of the flat plate solar collector (FPSC).

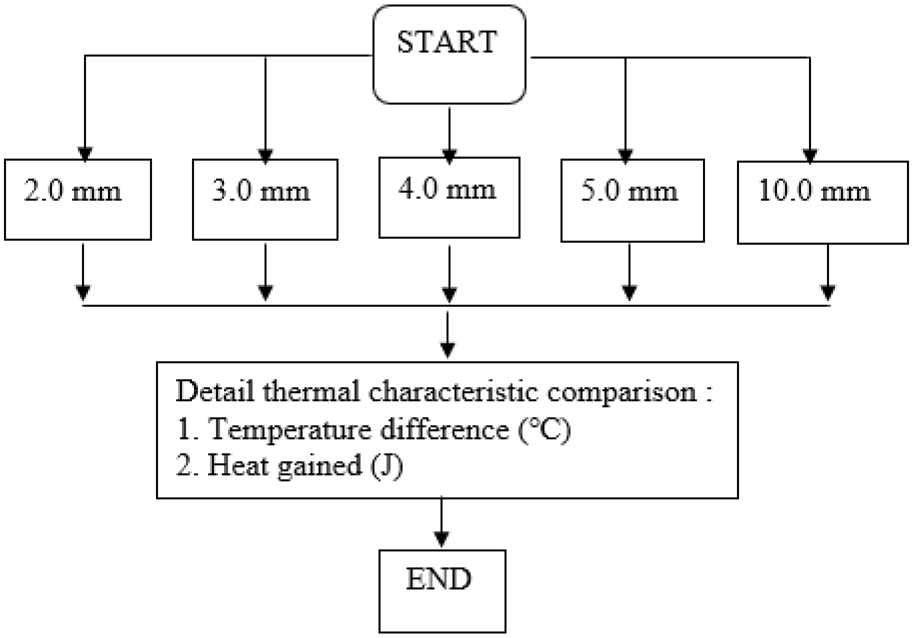

Fig. 8. Flow chart of the experiment with constant flat plate thickness and air-gap space

3.7 Evaluation Air Gap Distance (Between Flat Plate Absorber-Collector and Glass)

The thickness of the flat plate absorber and glass was used as the constant parameters in this experiment. Stainless steel 304 flat plate absorber thickness is 1.2 mm and the weight is 0.415 kg. Glass cover thickness of 2.0 mm was used for the flat plate solar collector. Solar simulator used in this experiment has 450 W/m^2 radiation. Figure 9 shows the process flow chart implemented in this work. The air gap distance of 0, 5.0, 10.0, 20.0, and 30.0 mm was applied for the air gap distance configuration in this experiment.

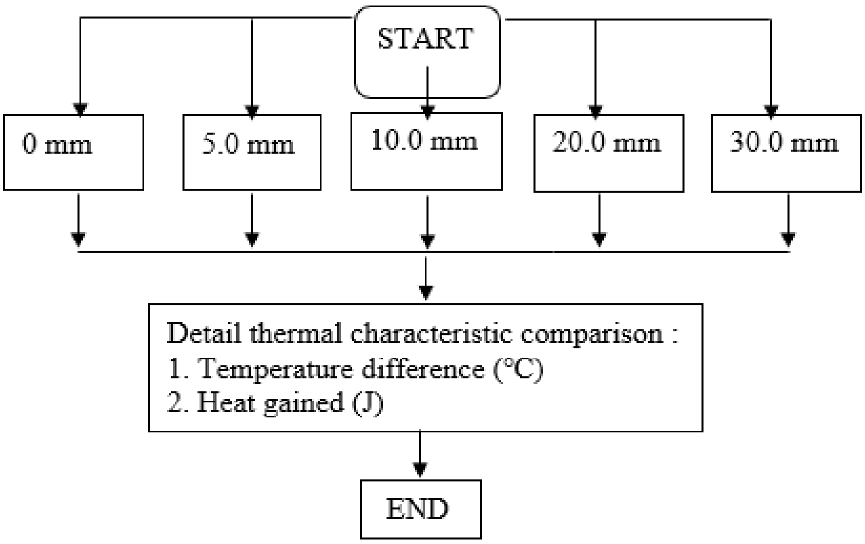

Fig. 9. Flow chart of the experiment with constant flat-plate absorber and glass thicknesses

3.8 Selection of Flat Plate Absorber Base Collector Thickness

Constant parameters used in this experiment were the glass thickness and air gap space, where the glass thickness was 2.0 mm, and the air gap distance was 10.0 mm. Solar radiation of 450 W/m^2 was applied in this experiment. Figure 10 presents the process flow chart of the experiment. Flat plate aluminum absorber base collector size applied in this experiment was 18.5 cm in width and 25.5 cm in length. Flat plate aluminum absorber base collector thickness and weight used in this experiment are 0.5 mm (0.073 kg), 0.8 (0.101 kg) mm, and 1.0 mm (0.119 kg).

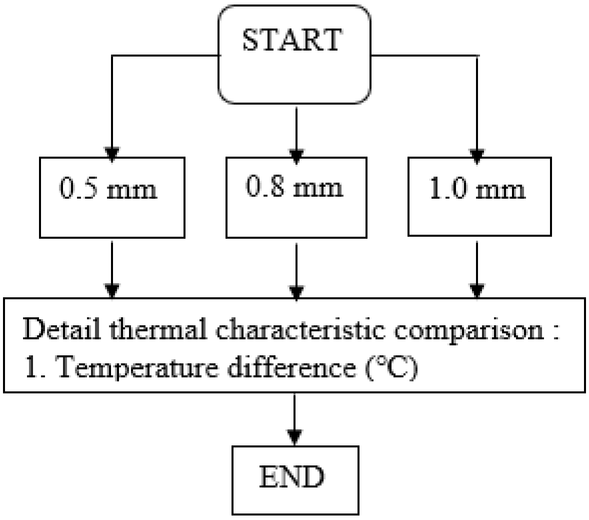

Fig. 10. Flow chart of the experiment with constant air-gap space and glass thickness

3.9 Double Glass as Glass Cover

Flat plate absorber thickness and glass thickness was used as constant parameters in this experiment. Stainless Steel 304 flate plate absorber thickness is 1.2 mm and its weight is 0.415 kg. Glass thickness of 2.0 mm was used as glass cover for flat plate solar collector. The radiation of the solar simulator was set at 450W/m^2. The air gap distance between flat plate absorber-collector and glass cover 1 is 10.0 mm. Figure 11 shows the double glass diagram for FPSC. The air gap distance between glass cover 1 and glass cover 2 is 0.4 mm.

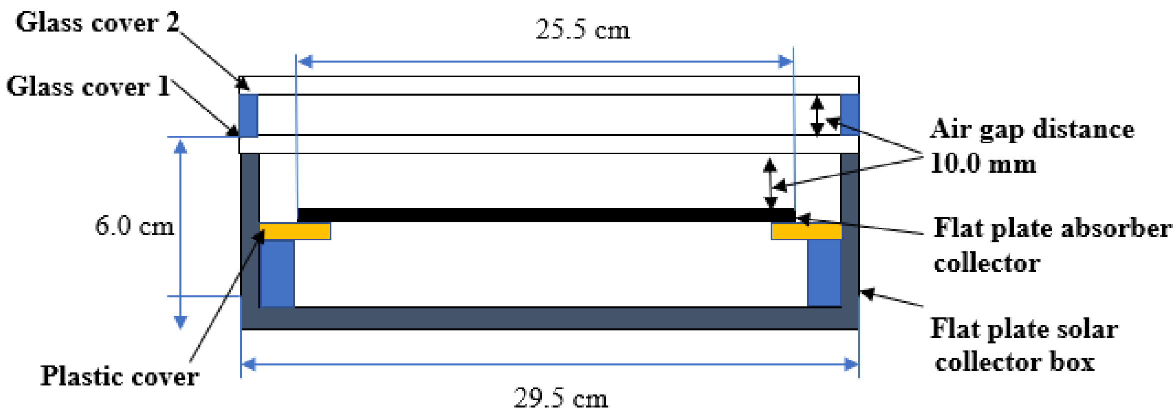

Fig. 11. Double glass diagram for the FPSC

4. Results and Discussion
4.1 Thermal Analysis

The heat transfer rate of the thermal absorber storage can be obtained from Eq. (6) [35]

$$Q_{Store} = \frac{m_{ab} C_{p(ab)} (T_2 - T_1)}{t_2 - t_1} \tag{6}$$

where,

m_{ab} = mass of thermal absorber (kg)
$C_{p(ab)}$ = specific heat of thermal absorber (kJ/kgK)
T_2 = temperature of thermal absorber after heat gain (K)
T_1 = temperature of thermal absorber before heat gain (K)
t_2 = time after heat gain (s)
t_1 = time before heat gain (s)

4.2 Materials Comparison

Figure 12 shows the flat plate absorber temperature versus time for different flat plate absorber materials. The aluminum flat plate absorber-collector responds rapidly in charging behavior than Stainless Steel 304 flat plate absorber. The aluminum and stainless-steel flat absorber have similar values of maximum temperature which is 66 °C at t = 600 seconds. Stainless steel has a higher temperature drop than aluminum flat plate absorber-collector in the discharging condition.

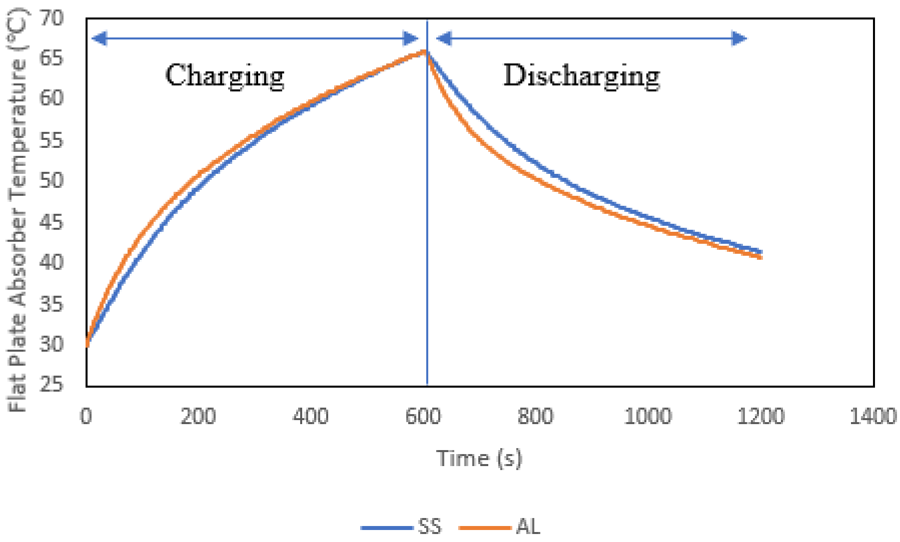

Fig. 12. Flat plate absorber temperature versus time for different flat plate absorber materials

Table 2 summarises the heat gain rate of different flat plate absorber-collector materials. The result shows that aluminum and stainless steel flat plate absorber-collectors have similar heat gain rate values which is 0.06 °C/s. Stainless steel flat plate absorber-collector has more advantage during discharging period, possessing more heat storage capability than aluminum flat plate absorber. The stainless steel flat plate absorber-collector is chosen as the flat plate absorber-collector.

Table 2
Summary of heat gain rate of different flat plate absorber-collector materials

Materials	Heat gain rate (̊C/s)	Maximum absorber temperature (̊C)
Aluminium	0.06	66.0
Stainless Steel	0.06	66.0

Figure 13 shows heat charging/heat discharging capacity versus different flat plate absorber material. Stainless Steel 304 flat plate absorber-collector has higher heat charging capacity (with a value of 4653.61 J) than Aluminium flat plate absorber capacity (with a value of 3283.31 J). Stainless Steel 304 flat plate absorber also has highest total heat gain which is 1499.50 J. Aluminium flat plate absorber-collector has lowest total heat gain at just 984.99 J. This result represents that Stainless Steel has high energy storage and could be used favourably with fluctuations of the solar radiation.

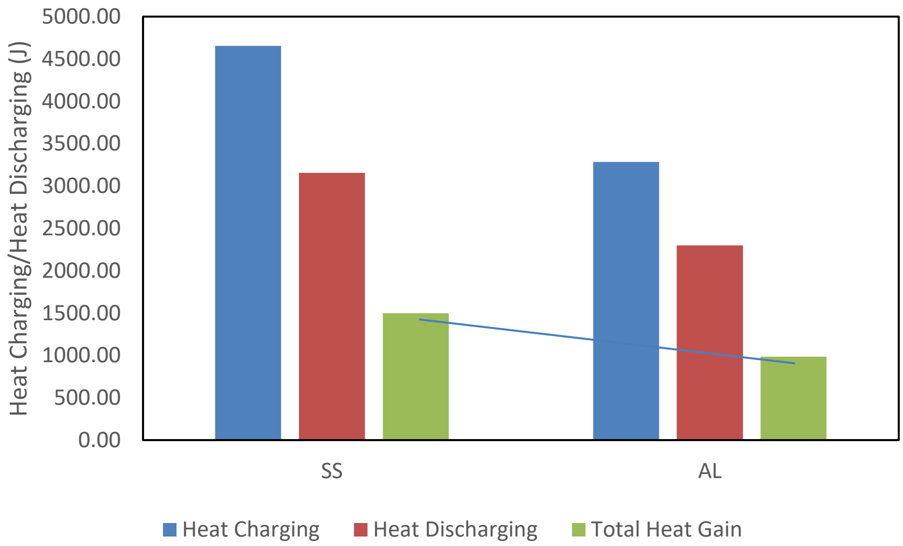

Fig. 13. Heat charging/ heat discharging versus different flat plate absorber materials

4.3 Coating Surface Comparison

Figure 14 presents the flat plate absorber temperature versus time for the coated and non-coated aluminum surfaces. A significant effect on the flat plate absorber temperature was noted on the surface coated with black paint. Based on the results, the aluminum-coated plate showed a fast response to the charging process and showed the highest flat plate absorber temperature of 85.8 °C at t = 300 seconds. Non-coated aluminum plate has maximum flat plate absorber temperature of 68.4°C at t = 300 seconds. During the discharging period aluminium-coated plate has higher temperature drop than non-coated aluminium.

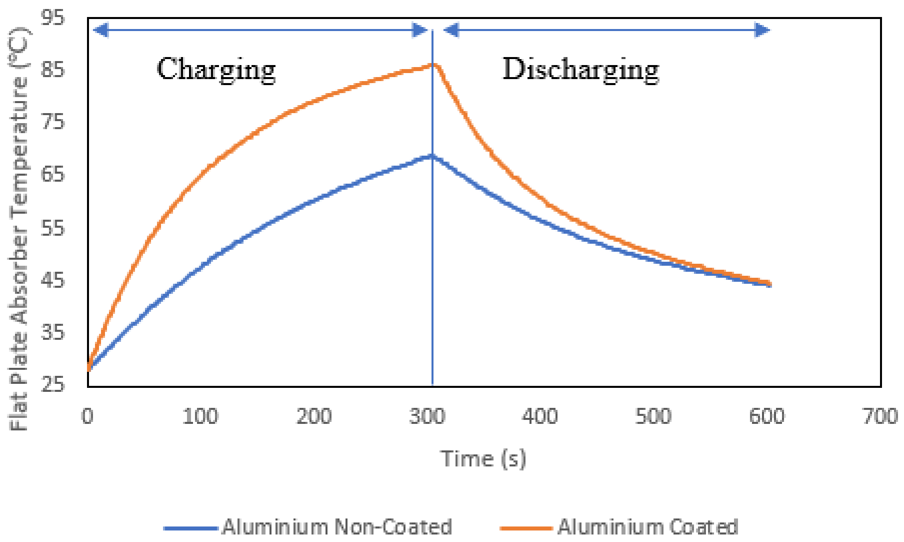

Fig. 14. Flat plate absorber temperature versus time for Aluminium coated and non-coated surface

Table 3 shows the summary of heat gain rate of aluminium coated and aluminium non-coated for flat plate absorber-collector material. The result shows that aluminium coated with matt black paint has higher heat gain rate which is 0.192 ℃/s than aluminium non-coated (0.136 ℃/s). It can be concluded that aluminium coated has absorbed high heat energy than aluminium non-coated. The flat plate absorber-collector surface should be coated with matt black coating to absorb high heat energy rate from solar radiation.

Table 3
Summary of heat gain rate and heat discharge rate of aluminium coated and aluminium non-coated

Materials	Heat gain rate (°C/s)	Maximum absorber temperature (°C)
Aluminium coated	0.192	85.8
Aluminium non-coated	0.136	68.4

4.4 Glass Thickness Comparison

Figure 15 shows the temperature behavior for different glass thicknesses. The results show that the flat plate absorber temperature configuration for 2.0 mm glass thickness has increased rapidly during the charging period. The flat plate absorber-collector of 2.0 mm glass thickness reached maximum temperature of 88.1°C at t = 600 seconds. The maximum temperatures of the flat plate absorber for glass thickness of 3.0 mm, 4.0 mm, 5.0 mm, and 10 mm gain temperature are 81.6 °C, 82.6 °C, 78.6 °C, and 70.5 °C, respectively, at t = 600 seconds.

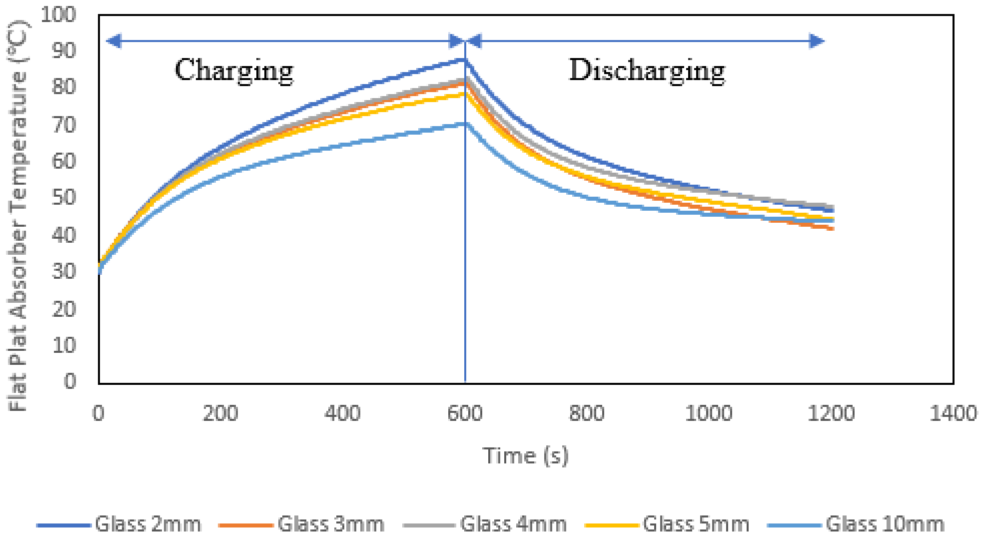

Fig. 15. Flat plate absorber temperature versus time for different glass thicknesses

Table 4 summarises the heat gain rate of different glass thicknesses. Glass thickness of 2.0 mm has a higher heat gain rate (0.097 °C/s) than other glass thickness configurations. The heat gain rate for glass thickness of 3.0 mm, 4.0 mm, 5.0 mm and 10.0 mm is 0.083 °C/s, 0.087 °C/s, 0.078 °C/s, and 0.067 °C/s, respectively. It can be concluded that during charging period flat plate absorber-collector for glass thickness 2.0 mm absorbs high heat energy than other glass thicknesses. The capability of 2.0 mm glass thickness provides more advantages to trap the heat loss from the flat plate absorber-collector.

Table 4
Summary of heat gain rate of different glass thicknesses

Glass Thickness (mm)	Heat gain rate (°C/s)	Maximum absorber temperature (°C)
2.0	0.097	88.1
3.0	0.083	81.6
4.0	0.087	82.6
5.0	0.078	78.6
10.0	0.067	70.5

Figure 16 presents the heat charging/heat discharging capacity versus glass thickness. The glass thickness of 2.0 mm has a higher heat charging capacity than other configurations at 3922.13 J. The lower heat charging occurs with glass thickness of 10.0 mm, at 2632.94 J. Glass thickness of 2.0 mm has the highest total heat gain which is 1207.33 J compared to other configurations. It can be concluded that by increasing the glass thickness, the total heat gain will be reduced [36]. The 2.0 mm thick glass also has higher transmittance than other configurations. The flat plate absorber-collector can absorb high heat energy from solar radiation.

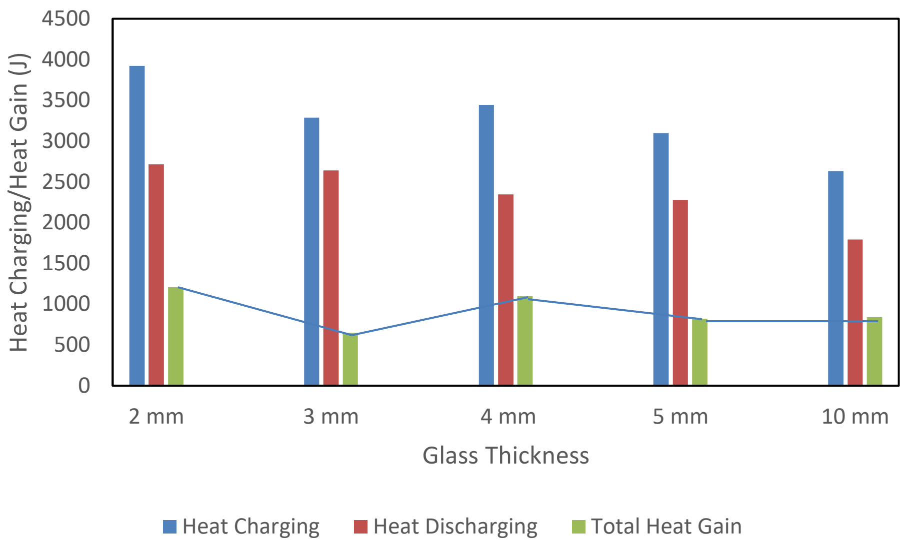

Fig. 16. Heat charging/ heat discharging versus glass thickness

4.5 Optimum of Air Gap Thickness (Between Flat Plate Absorber and Glass)

The parameters used in this experiment for the air gap thickness are 0, 5.0, 10.0, 20.0, and 30.0 mm. Figure 17 shows the temperature behavior of the air gap thickness in the flat plate absorber-collector. During the initial stage of the charging period, the flat plate absorber temperature for air gap distance of 10.0 mm increased rapidly. The air gap distance achieved maximum temperature of 64.6 °C at t = 600 s. The 0, 5.0, 20.0, and 30.0 mm air gap distance showed the maximum flat plate absorber temperature of 59.1 °C, 62.4 °C, 60.9 °C, 60.6 °C at t = 600 seconds. The temperature drop for air gap thickness of 10.0 mm is slightly higher for the discharging period than for other air gap thickness configurations. It can be concluded that the flat plate absorber-collector temperature varies with different configurations of air gap thickness [37].

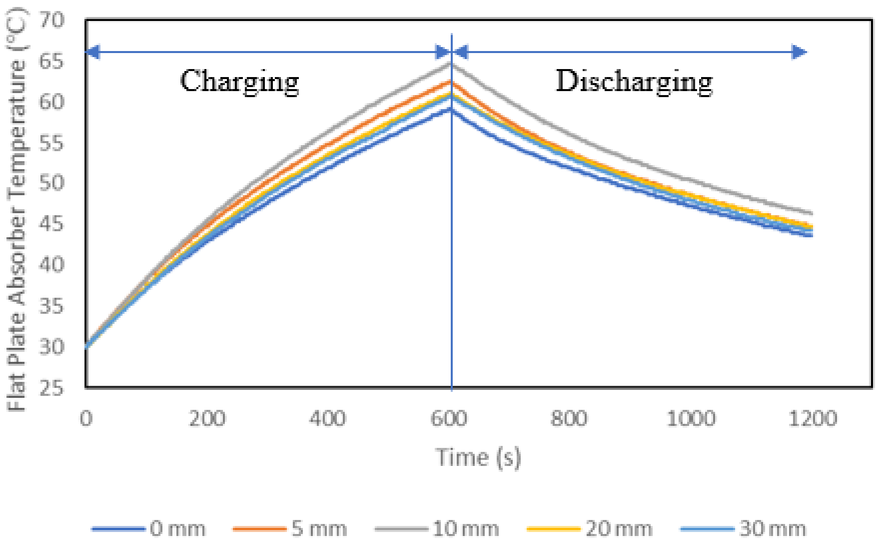

Fig. 17. Flat plate absorber temperature versus time for air gap space between flat plate absorber and glass

Table 5 summarises the heat gain rate of air gap space between the absorber and glass. The air gap space of 10.0 mm has a higher heat gain rate (0.058 ℃/s) than other air gap configurations. The heat gain rate for 0, 5.0, 20.0, and 30.0 mm air gap thickness yield values of temperature increase of 0.049 ℃/s, 0.054 ℃/s, 0.052 ℃/s, and 0.051 ℃/s, respectively. Air gap space of 10.0 mm shows the optimum performance in term of charging period for flat plate absorber-collector to gain high heat energy from solar radiation. Hence, 10.0 mm air gap thickness is select as the optimum design parameter for FPBTCA.

Table 5
Summary of heat gain rate and heat discharge rate of air gap distance between flat plate absorber and glass

Gap distance (mm)	Heat gain rate (̊C/s)	Maximum absorber temperature (̊C)
0	0.049	59.1
5.0	0.054	62.4
10.0	0.058	64.6
20.0	0.052	60.9
30.0	0.051	60.6

Figure 18 shows the heat charging/heat discharging capacity versus the air gap thickness between the absorber and glass. The highest heat charging capacity occurs when the air gap distance is 10.0 mm, at 6770.06 J. Meanwhile, the lowest heat charging is noted at air gap thickness of 0 mm, which is 5641.72 J. The highest total heat gain is 4750.92 J at air gap thickness of 10.0 mm. It can be concluded that air gap thickness of 10.0 mm between flat plate absorber and glass stores high heat energy in the flat plate absorber-collector than other configurations.

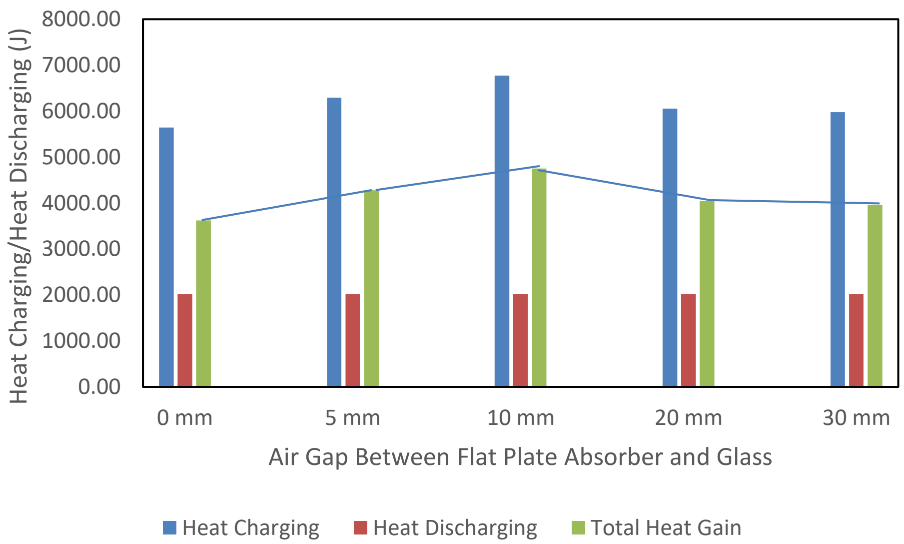

Fig. 18. Heat charging/ heat discharging versus air gap between absorber-collector and glass

4.6 Flat Plate Thermal Cell Absorber

Figure 19 presents the stainless steel 304 flat plate absorber temperature versus time for different flat plate thermal cell absorbers. The results show that the stainless steel flat plate absorber-collector temperature with 1.0 mm thickness changed rapidly to the charging period. The

1.0 mm stainless steel plate has a higher flat plate absorber-collector temperature of 76.2 ℃ at t = 600 seconds. Meanwhile, the maximum temperature of flat plate absorber temperature at t = 600 seconds for the 0.5 mm thickness is 68.6 ℃ and 66 ℃ for the 2.0 mm thickness.

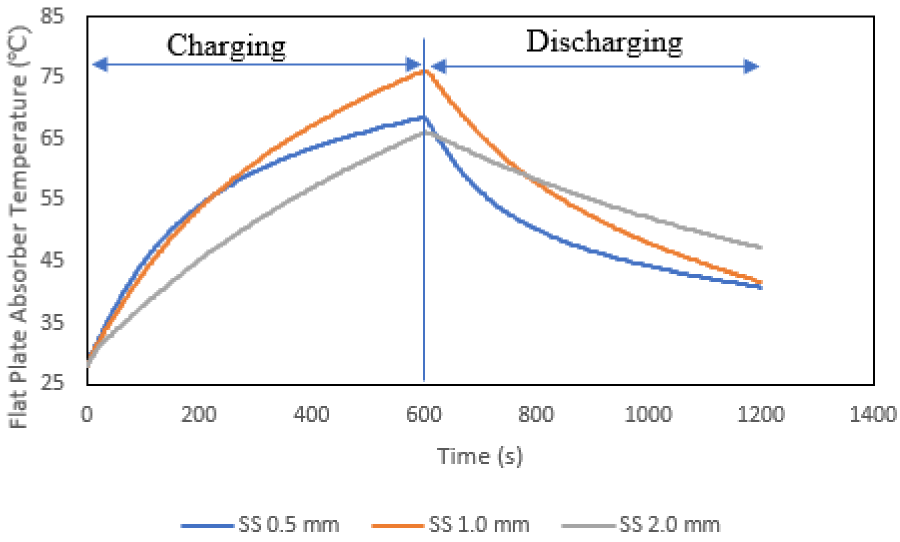

Fig. 19. Flat plate absorber temperature versus time for different Stainless Steel 304 flat plate thermal cell absorber

Table 6 summarises the heat gain rate of different Stainless Steel 304 flat plate thermal cell absorbers. The flat plate thermal cell absorber of 1.0 mm thickness has a higher heat gain rate which is 0.080 °C/s compared to other configurations. The heat gain rate for the flat plate thermal cell absorber of 0.5 mm and 2.0 mm thickness is 0.067 °C/s and 0.063 °C/s. Stainless steel 1.0 mm absorbs high heat energy during charging period than other configurations. Based on the result, the thickness of 1.0 mm is preferred as the flat plate thermal cell absorber for FPBTCA.

Table 6
Summary of heat gain rate of different Stainless Steel 304 flat plate thermal cell absorber

SS thickness (mm)	Heat gain rate (̊C/s)	Maximum absorber temperature (̊C)
0.5	0.067	68.6
1.0	0.080	76.2
2.0	0.063	66.0

4.7 Flat Plate Absorber Base Collector

Aluminum flat plate absorber thicknesses of 0.5, 0.8, and 1.0 mm are used in this experiment. The experimental results are presented in Figure 20, showing the temperature behavior of different flat plate absorber thicknesses. During the initial stage of the charging period, the temperature of the Aluminium 0.5 mm thickness increases rapidly. Meanwhile, the flat plate absorber of 0.5 mm achieves maximum temperature of 67.2 °C at t = 600 seconds. In contrast, the plate thickness of 0.8 and 1.0 mm achieves maximum temperature of 66.0 and 64.7 °C, respectively, at t= 600 seconds. This indicates that the geometry [38] of the flat plate absorber-collector could affect the performance of the flat plate solar collector.

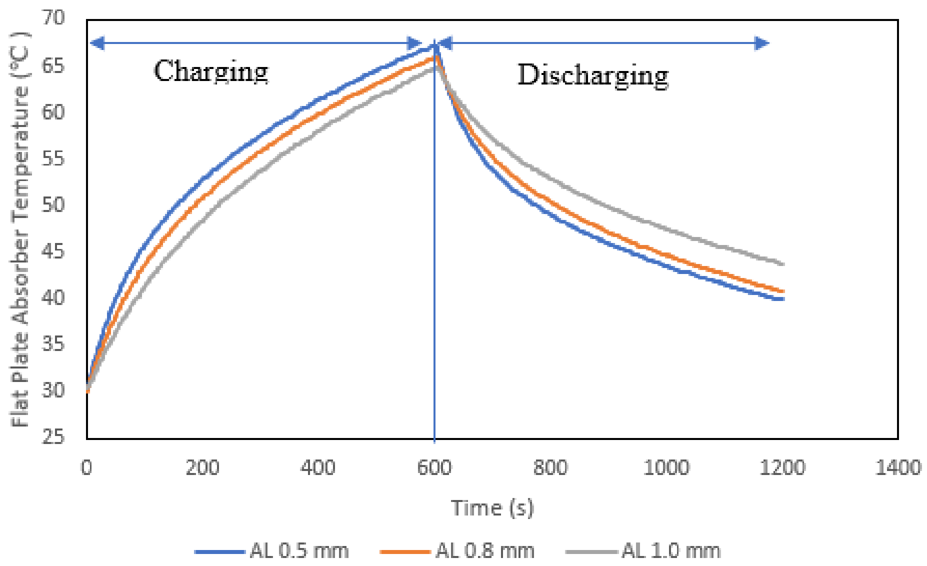

Fig. 20. Flat plate absorber temperature versus time for different flat plate absorber base collector thicknesses

Table 7 summarises the heat gain rate of different flat plate absorber base collector thicknesses. The heat gain rate for the aluminium flat plate absorber base of 0.5 mm thickness shows the highest temperature than other configurations, with the value of 0.062 °C/s. Meanwhile, the heat gain rates for the aluminium flat plate absorber base collector with 0.8 mm and 1.0 mm thickness are 0.060 °C/s and 0.057 °C/s. It show aluminium 0.5 mm absorbed high heat energy during charging period than other configurations, respectively. Aluminium 0.5 mm thickness is selected as design parameter for FPBTCA.

Table 7
Summary of heat gain rate of different flat plate absorber base collector thicknesses

Absorber thickness (mm)	Heat gain rate (°C/s)	Maximum absorber temperature (°C)
0.5	0.062	67.2
0.8	0.060	66.0
1.0	0.057	64.7

4.8 Glass Cover Comparison

Figure 21 represents flat plate absorber temperature versus time for different glass cover comparison. Double glass shows the highest flat plate absorber-collector temperature than single glass which is 76.3 °C, at t= 600 seconds. Maximum temperature of flat plate absorber temperature at t = 600 seconds for single glass configuration is 73.2 °C. Double glass configuration also has higher temperature drop than single glass. The result also indicates that double glass as glass cover for flat plate solar collector could generate lower top loss on heat transfer coefficient than single glass configuration [39].

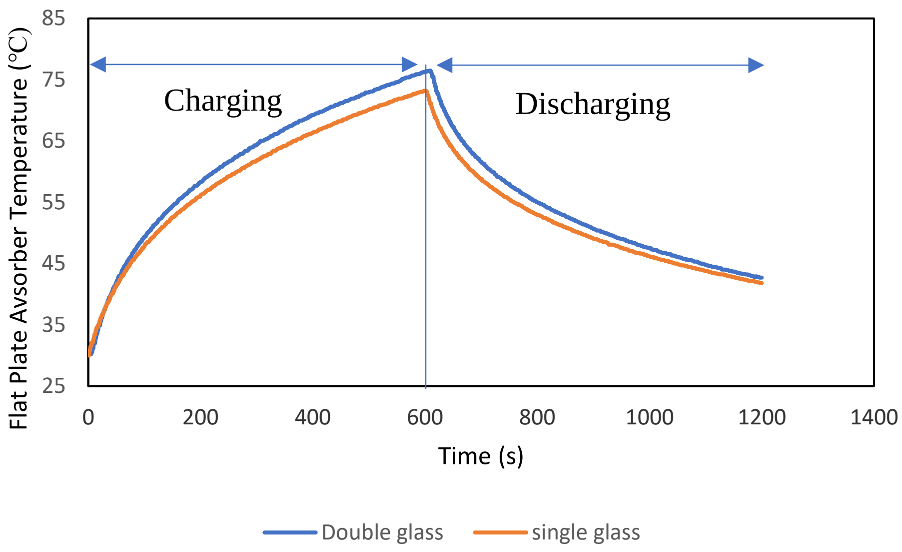

Fig. 21. Flat plate absorber temperature versus time for different glass cover comparison

Table 8 summarizes the heat gain rate of different glass covers. The highest heat gain rate is double glass with a value of 0.077 °C/s. Meanwhile, the heat gain rate for the single glass is 0.072 °C/s. It can be concluded that flat plate absorber-collector for double glass configuration absorbs high heat energy during the charging period from solar radiation as compared to single glass configuration. Hence, double glass as glass cover is selected as the design parameter for FPBTCA.

Table 8
Summary of heat gain rate of different glass covers

Glass cover	Heat gain rate (̊C/s)	Maximum absorber temperature (̊C)
Single glass	0.072	73.2
Double glass	0.077	76.3

5. Design Parameters for Flat Plate Base-Thermal Cell Absorber (FPBTCA)

Several design parameters had been determined in this study. However, this research had been specially designed to achieve the highest performance of a Flat Plate Base-Thermal Cell Absorber (FPBTCA) present performance. Table 9 lists the chosen design parameters of the Flat Plate Base-Thermal Cell Absorber (FPBTCA). The design parameters selected are based on the optimum performance of the flat plate solar collector. Figure 22 shows the FPBTCA diagram. The flat plate absorber base collector is combined with thermal cell absorber in one unit. This design is applicable for solar radiation more than 200 W/m^2 and for raining time it will not been operate well. During normal or good sunshine period the solar collector can work from 9.00 am to 6.00 pm. The flat plate solar collector will produce higher energy gain with larger surface area, but the temperature will remain due to surface area of the absorber-collector exposed to solar radiation. The selection done is to obtained flat plate solar collector with thermal cell absorber for small energy gain application.

Table 9
Chosen design parameters for Flat Plate Base-Thermal Cell Absorber (FPBTCA)

Design parameter	Parameters
Coating surface	Matt black coating
Air gap between flat plate absorber collector and glass cover 1	10.0 mm
Air gap between glass cover 1 and glass cover 2	0.4 mm
Thermal cell absorber (10 cm x 10 cm)	Stainless Steel 1.0 mm
Flat plate base absorber (18.5 cm x 25.5 cm)	Aluminium 0.5 mm
Glass thickness	2.0 mm

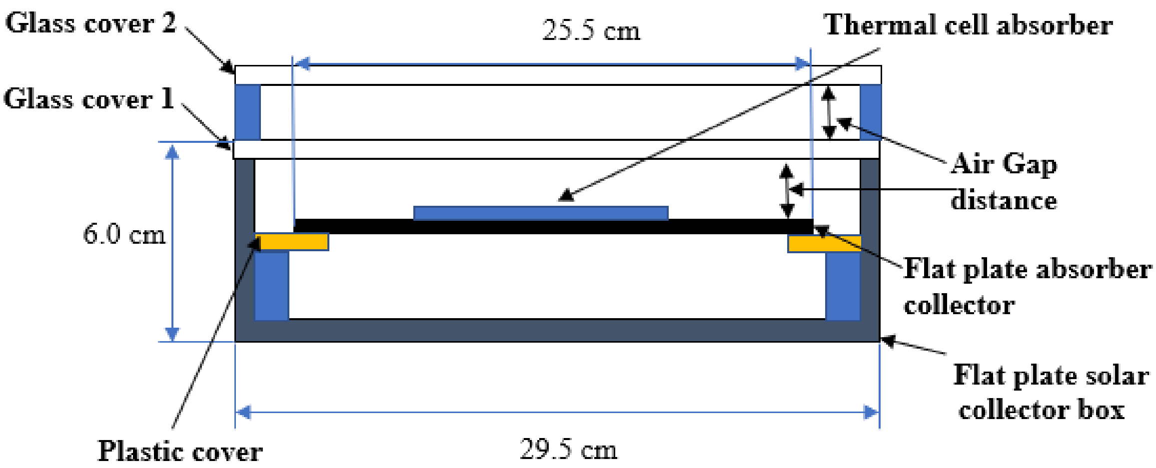

Fig. 22. Flat Plate Base-Thermal Cell Absorber (FPBTCA) diagram

6. Conclusion

The design parameters considered in this study are flat plate absorber materials, different glass thicknesses, air gap distance, thermal cell absorber thickness, and flat plate absorber base collector thickness. This study had focused on the selection of optimum design parameters for designing a portable Flat Plate Base-Thermal Cell Absorber (FPBTCA). The experimental data were compared graphically using Microsoft Excel. Several conclusions are deduced based on the experimental outcome

i. The design parameters chosen, such as flat plate absorber materials and thicknesses, different glass thicknesses, and air gap distance (or space), could significantly affect the flat plate absorber-collector temperature increase.
ii. The design parameter of 10 mm air gap distance and 2.0 mm glass thickness have been selected as providing the most optimum performance for the FPBTCA design.
iii. Stainless Steel 304 flat plate absorber-collector of 1.0 mm thickness has been chosen for the FPBTCA absorber thermal cell due to its fast response to the charging process and its capability to store the absorbed heat.
iv. Aluminium 0.5 mm thickness is suitable to be used as the material for the FPBTCA flat plate absorber base collector based on its fast-charging performance and higher thermal conductivity than stainless steel.
v. Double glass configuration has shown optimum flat plate absorber temperature increase as compared to single glasss configuration.

7. Recommendations

In future this research could further be extended to develope efficient thermal cell absorber by optimising surface area size and material used for flat plate solar collector performance enhancement. This may produce efficient Flat Plate Base-Thermal Cell Absorber (FPBTCA).

Acknowledgements
The authors wish to express their grateful acknowledgement to Kulliyyah of Engineering (KOE) and Kulliyyah of Allied Health Sciences (KAHS), International Islamic University Malaysia (IIUM) together with Solar Energy Research Institute, National University of Malaysia (SERI-UKM) for the use of laboratory facilities, as well as MRUN Research Grant (RU-2019-001/1) and RADTEC Enterprise for the financial support.

References
[1] Bahadori, Alireza, and Chikezie Nwaoha. "A review on solar energy utilisation in Australia." *Renewable and Sustainable Energy Reviews* 18 (2013): 1-5. https://doi.org/10.1016/j.rser.2012.10.003
[2] Panwar, N. L., S. C. Kaushik, and Surendra Kothari. "Role of renewable energy sources in environmental protection: A review." *Renewable and sustainable energy reviews* 15, no. 3 (2011): 1513-1524. https://doi.org/10.1016/j.rser.2010.11.037
[3] Timilsina, Govinda R., Lado Kurdgelashvili, and Patrick A. Narbel. "Solar energy: Markets, economics and policies." *Renewable and sustainable energy reviews* 16, no. 1 (2012): 449-465. https://doi.org/10.1596/1813-9450-5845
[4] Prasad, Ram, Sri Sivakumar, Umesh Chandra Sharma, and J. N. Govil. "ENERGY SCIENCE AND TECHNOLOGY." (2015).
[5] El-Sebaii, A. A., and S. M. Shalaby. "Solar drying of agricultural products: A review." *Renewable and Sustainable Energy Reviews* 16, no. 1 (2012): 37-43. https://doi.org/10.1016/j.rser.2011.07.134
[6] Musembi, Maundu Nicholas, Kosgei Sam Kiptoo, and Nakajo Yuichi. "Design and analysis of solar dryer for mid-latitude region." *Energy procedia* 100 (2016): 98-110. https://doi.org/10.1016/j.egypro.2016.10.145
[7] Yahaya, M. "Design and performance evaluation of a solar assisted heat pump dryer integrated with biomass furnace for red chili." *Int. J. Photoenergy* (2016): 1-14. https://doi.org/10.1155/2016/8763947
[8] Kumar, Mahesh, Sunil Kumar Sansaniwal, and Pankaj Khatak. "Progress in solar dryers for drying various commodities." *Renewable and Sustainable Energy Reviews* 55 (2016): 346-360. https://doi.org/10.1016/j.rser.2015.10.158
[9] Aral, Serdar, and Ayşe Vildan Beşe. "Convective drying of hawthorn fruit (Crataegus spp.): Effect of experimental parameters on drying kinetics, color, shrinkage, and rehydration capacity." *Food chemistry* 210 (2016): 577-584. https://doi.org/10.1016/j.foodchem.2016.04.128
[10] Colangelo, Gianpiero, Ernani Favale, Paola Miglietta, and Arturo de Risi. "Innovation in flat solar thermal collectors: A review of the last ten years experimental results." *Renewable and Sustainable Energy Reviews* 57 (2016): 1141-1159. https://doi.org/10.1016/j.rser.2015.12.142
[11] Verma, Sujit Kumar, Arun Kumar Tiwari, Sandeep Tiwari, and Durg Singh Chauhan. "Performance analysis of hybrid nanofluids in flat plate solar collector as an advanced working fluid." *Solar Energy* 167 (2018): 231-241. https://doi.org/10.1016/j.solener.2018.04.017
[12] Jamil, Muhammad Mahmud, Nor Azwadi Che Sidik, and Siti Nurul Akmal Yusof. "Solar Collector Application using Nanofluid in Thermosyphon." *Journal of Advanced Research in Materials Science* 65, no. 1 (2020): 1-15. https://doi.org/10.37934/arms.65.1.115
[13] Tian, Yuan, and Chang-Ying Zhao. "A review of solar collectors and thermal energy storage in solar thermal applications." *Applied energy* 104 (2013): 538-553. https://doi.org/10.1016/j.apenergy.2012.11.051
[14] Karsli, Suleyman. "Performance analysis of new-design solar air collectors for drying applications." *Renewable Energy* 32, no. 10 (2007): 1645-1660. https://doi.org/10.1016/j.renene.2006.08.005
[15] Essalhi, Hajar, Rachid Tadili, and Mohammed Najib Bargach. "Comparison of thermal performance between two solar air collectors for an indirect solar dryer." *Journal of Physical Science* 29, no. 3 (2018): 55-65. https://doi.org/10.21315/jps2018.29.3.5
[16] Kalogirou, Soteris A. "Progress in energy and combustion science." *Prog. Ener. Combust. Sci* 30 (2004): 231-295. https://doi.org/10.1016/j.pecs.2004.02.001

[17] Billy, Anak Sup, Tanti Zanariah Shamshir Ali, Mohd Farid Zainudin, and Abu Bakar Rosli. "Experimental Study of Water Heating Efficiency Between Aluminium and Copper Absorber Plate in Solar Flat Plate Collector." In *Applied Mechanics and Materials*, vol. 660, pp. 709-713. Trans Tech Publications Ltd, 2014. https://doi.org/10.4028/www.scientific.net/AMM.660.709
[18] Syuhada, Ahmad, and Muhammad Ilham Maulana. "Absorber Thickness Effect on The Effectiveness of Solar Collectors to Production Hot Air For Drying." In *E3S Web of Conferences*, vol. 67, p. 04028. EDP Sciences, 2018. https://doi.org/10.1051/e3sconf/20186704028
[19] Sup, Billy. "Effect of Absorber Plate Material on Flat Plate Collector Efficiency." PhD diss., UMP, 2010.
[20] Kang, Myeong-Cheol, Yong-Heack Kang, Sang-Hoon Lim, and Wongee Chun. "Numerical analysis on the thermal performance of a roof-integrated flat-plate solar collector assembly." *International Communications in Heat and Mass Transfer* 33, no. 8 (2006): 976-984. https://doi.org/10.1016/j.icheatmasstransfer.2006.04.013
[21] Ion, I. V., and Jorge G. Martins. "Design, developing and testing of a solar air collector." *The annals of "Dunarea de Jos."* *University of Galati* (2006): 72-76.
[22] Bakari, Ramadhani, Rwaichi JA Minja, and Karoli N. Njau. "Effect of glass thickness on performance of flat plate solar collectors for fruits drying." *Journal of energy* 2014 (2014). https://doi.org/10.1155/2014/247287
[23] Ghoneyem, Abdulrahman, and Arif Ileri. "Software to analyze solar stills and an experimental study on the effects of the cover." *Desalination* 114, no. 1 (1997): 37-44. https://doi.org/10.1016/S0011-9164(97)00152-5
[24] Dheyab, Hussam S., Manar Salih Mahdi Al-Jethelah, Tadahmun Ahmed Yassen, and Thamir Khalil Ibrahim. "Experimental study of the optimum air gap of a rectangular solar air heater." *Journal of Advanced Research in Fluid Mechanics and Thermal Sciences* 59, no. 2 (2019): 318-329.
[25] Subiantoro, Alison, and Kim Tiow Ooi. "Analytical models for the computation and optimization of single and double glazing flat plate solar collectors with normal and small air gap spacing." *Applied energy* 104 (2013): 392-399. https://doi.org/10.1016/j.apenergy.2012.11.009
[26] Do Ango, AC Mintsa, Marc Médale, and Chérifa Abid. "Optimization of the design of a polymer flat plate solar collector." *Solar Energy* 87 (2013): 64-75. https://doi.org/10.1016/j.solener.2012.10.006
[27] Manikandan, J., and B. Sivaraman. "Comparative studies on thermal efficiency of single and double glazed flat plate solar water heater." *ARPN Journal of engineering and applied sciences* 11, no. 9 (2016): 5521-5526.
[28] Youcef-Ali, Sabri. "Study and optimization of the thermal performances of the offset rectangular plate fin absorber plates, with various glazing." *Renewable Energy* 30, no. 2 (2005): 271-280. https://doi.org/10.1016/j.renene.2004.04.009
[29] Abu-Hamdeh, Nidal H., Rashad AR Bantan, Morteza Khoshvaght-Aliabadi, and Ashkan Alimoradi. "Effects of ribs on thermal performance of curved absorber tube used in cylindrical solar collectors." *Renewable Energy* 161 (2020): 1260-1275. https://doi.org/10.1016/j.renene.2020.07.077
[30] Kumar, Rakesh, and Marc A. Rosen. "Thermal performance of integrated collector storage solar water heater with corrugated absorber surface." *Applied Thermal Engineering* 30, no. 13 (2010): 1764-1768. https://doi.org/10.1016/j.applthermaleng.2010.04.007
[31] Kürklü, Ahmet, Aziz Özmerzi, and Sefai Bilgin. "Thermal performance of a water-phase change material solar collector." *Renewable Energy* 26, no. 3 (2002): 391-399. https://doi.org/10.1016/S0960-1481(01)00130-6
[32] Anirudh, K., and S. Dhinakaran. "Numerical study on performance improvement of a flat-plate solar collector filled with porous foam." *Renewable Energy* 147 (2020): 1704-1717. https://doi.org/10.1016/j.renene.2019.09.038
[33] Hussein, Ahmed Kadhim. "Applications of nanotechnology to improve the performance of solar collectors–Recent advances and overview." *Renewable and Sustainable Energy Reviews* 62 (2016): 767-792. https://doi.org/10.1016/j.rser.2016.04.050
[34] Choudhury, C., P. M. Chauhan, and H. P. Garg. "Performance and cost analysis of two-pass solar air heaters." *Heat recovery systems and CHP* 15, no. 8 (1995): 755-773. https://doi.org/10.1016/0890-4332(95)00003-H
[35] John, W. A. B., and A. Duffie. "Wiley: Solar Engineering of Thermal Processes." (2013). https://doi.org/10.1002/9781118671603
[36] Ismail, K. A. R., and J. R. Henríquez. "Modeling and simulation of a simple glass window." *Solar energy materials and solar cells* 80, no. 3 (2003): 355-374. https://doi.org/10.1016/j.solmat.2003.08.010
[37] Ferahta, F. Z., S. Bougoul, D. Ababsa, and C. Abid. "Numerical study of the convection in the air gap of a solar collector." *Energy Procedia* 6 (2011): 176-184. https://doi.org/10.1016/j.egypro.2011.05.021
[38] Manikandan, J., and B. Sivaraman. "Experimental analysis of double glazed flat plate solar water heater with various absorber plate geometries." *International Energy Journal* 15, no. 4 (2016).
[39] Vettrivel, H., and Palanivel Mathiazhagan. "Comparison study of solar flat plate collector with single and double glazing systems." *International Journal of Renewable Energy Research (IJRER)* 7, no. 1 (2017): 266-274.